
Technical Paper

Journal of the Society of
Naval Architects of Korea
Vol. 27, No. 1, March 1990
大韓造船學會誌
第27卷 第1號 1990年 3月

Nonlinear Effects on the Cable Dynamic Behaviour

by

Hyunkyong Shin*

케이블의 동적거동에 미치는 비선형 영향

신 현 경*

ABSTRACT

The effects on the dynamic behaviour of the geometric nonlinearity and large dynamic tensile forces occurring in hostile sea environments must be investigated for assessing extreme tensions and fatigue life expectancy of cable.

In this paper, the combined effects on the cable dynamic responses are shown through comparisons between numerical solutions to the cable dynamic equations with geometric nonlinearity and large tensile force terms as well as nonlinear drag term and those to the cable equations with only nonlinear drag term.

It is found that, in steady state, the combined effects increase the maximum dynamic tension and reduce the magnitude of the minimum of the dynamic tension at the middle of the cable. This decrease together with the increase of the maximum dynamic tension, cause the average tension to become higher and, therefore, it may deteriorate the cable fatigue life.

요 약

거친 해상에서 케이블에 형성될 수 있는 큰 동장력(large dynamic tensile forces)과 기하학적 비선형성(geometric nonlinearity)의 고려는 비선형 케이블 운동방정식(nonlinear cable dynamics)의 해에 상당한 영향을 끼치며 이 결과의 응용은 케이블의 극단장력(extreme tensions)과 slack-and-snapping 케이블의 연구에서 필수적인 부분이 될 것이다. 비선형 유체항력만을 포함한 경우와 기하학적 비선형성과 큰 동장력항을 함께 포함하는 경우의 케이블 운동방정식의 해를 비교하여, 케이블의 동적 거동에 대한 기하학적 비선형과 큰 동장력항의 복합적인 영향을 연구한다.

큰 동장력항과 기하학적 비선형성의 고려는, 최대 동장력의 증가를 가져오나 반면에 최소 동장력의 크기에서의 감소를 가져옴으로, 결국 동장력의 평균값의 상승과 그로인한 케이블의 피로수명 단축을 유발할 수 있다.

발표 : 1989년 대한조선학회 추계연구발표회('89.11.11)

Manuscript received : December 1, 1989, revised manuscript received : Jan. 23, 1990

* Member, University of Ulsan

1. Introduction

Two typical offshore applications, deeper water moorings and open sea towing, suffer from very large cable dynamic tension amplification in rough seas, necessitating a detailed analysis.[1] This in turn requires a complete understanding of the effect of the nonlinearities involved.[2]

Author has studied the combined effects of the geometric nonlinearity, large dynamic tension and nonlinear drag forces on the cable dynamic response, with the limitation that the total tension remains positive at all times.[5] For the analysis of nonlinear effects on cable dynamics, great attention is paid to the time domain simulation methods. The time domain simulation method employed here is based on the collocation method spatially and Newmark's method for time integration.[4] and [5]

The numerical applications are made and through comparison between the dynamic response of the cable with only nonlinear drag forces and that of the cable with the combined effects of geometric nonlinearity and large tensile forces, author find that, in steady state, the combined effects increase the maximum dynamic tension and reduce the magnitude of the minimum of the dynamic tension.

2. Simplified Nonlinear Governing Equations

The 2-dimensional, simplified nonlinear equations of motion of a cable with coplanar static configuration, expressed along the local tangential and normal directions are.[1], [2], [5]

$$\begin{aligned}
 m \frac{\partial^2 p}{\partial t^2} &= \frac{\partial T_1}{\partial s} - T_0 \frac{d\phi_0}{ds} \phi_1 + [F_{t1} - F_{n1} \phi_1](1+e) \\
 &\quad - F_{t0}(1+e_0) + m_a \frac{\partial^2 q}{\partial t^2} \phi_1 - T_1 \frac{d\phi_0}{ds} \phi_1 \\
 (m+m_a) \frac{\partial^2 q}{\partial t^2} &= -\frac{dT_0}{ds} \phi_1 + T_0 \frac{\partial \phi_1}{\partial s} + T_1 \frac{d\phi_0}{ds} \\
 &\quad + [F_{t1} \phi_1 + F_{n1}](1+e) - F_{n0}(1+e_0) \\
 &\quad + \frac{\partial T_1}{\partial s} \phi_1 + T_1 \frac{\partial \phi_1}{\partial s} \\
 EA \frac{\partial p}{\partial s} - EAq \frac{d\phi_0}{ds} &= EA(1+e) \left(-\frac{\phi_1^2}{2} \right) + EAe_1
 \end{aligned}$$

$$EA \frac{\partial q}{\partial s} + EA p \frac{d\phi_0}{ds} = EA(1+e)\phi_1 \quad (1 \text{ a, b, c, d})$$

where

- T_0 : static effective tension
- T_1 : dynamic effective tension
- p : tangential displacement based on the static configuration
- q : normal displacement based on the static configuration
- s : Lagrangian coordinate
- ϕ_0 : static angle
- ϕ_1 : dynamic angle
- e_0 : static strain
- e_1 : dynamic strain ($e=e_0+e_1$)
- m : mass per unit length
- m_a : added mass per unit length ($M=m+m_a$)
- E : Young's modulus
- A : cable sectional area
- $F_{t1}(F_{t0})$: tangential component of the fluid drag force based on the moving (static) configuration of the cable.
- $F_{n1}(F_{n0})$: normal component of the fluid drag force based on the moving (static) configuration of the cable.

The first two equations express the force equilibrium in the tangential and normal directions based on the static configuration respectively; the next two equations express compatibility of motion.

From equations (1a,b,c,d), we identify the following nonlinear terms.

$$\begin{aligned}
 &m_a \frac{\partial^2 q}{\partial t^2} \phi_1 \text{ and } T_1 \frac{d\phi_0}{ds} \phi_1 \\
 &\frac{\partial T_1}{\partial s} \phi_1 \text{ and } T_1 \frac{\partial \phi_1}{\partial s} \\
 &(1+e) \left(-\frac{\phi_1^2}{2} \right) \\
 &e\phi_1 \\
 &\text{Nonlinear drag terms} \quad (2a, b, c, d, e)
 \end{aligned}$$

Boundary conditions and Initial conditions are as follows (Fig. 1).

- Boundary conditions

$$\begin{aligned}
 p(0, t) &= 0 \\
 q(0, t) &= 0 \\
 p(1, t) &= h(t) \cos(\phi_{0top} - \theta) \\
 q(1, t) &= -h(t) \sin(\phi_{0top} - \theta)
 \end{aligned} \quad (3)$$

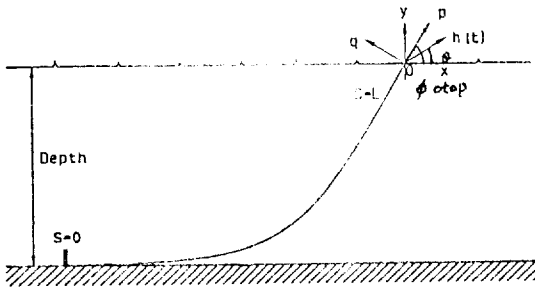


Fig. 1 Excitation and Lagrangian Coordinates

Where

$h(t)$: arbitrary excitation function of time t imposed at the top of the cable.

ϕ_{0top} : static angle at the top of the cable

θ : angle of direction of the excitation

• Initial conditions

$$p(s, 0) = f_1(s)$$

$$q(s, 0) = f_2(s)$$

$$\frac{\partial p}{\partial t}(s, 0) = f_3(s)$$

$$\frac{\partial q}{\partial t}(s, 0) = f_4(s) \tag{4}$$

where $f_1(s)$, $f_2(s)$, $f_3(s)$ and $f_4(s)$ are arbitrary functions of the Lagrangian coordinates.

For the numerical scheme, we employ an expansion of the response in terms of Chebyshev polynomials [4]; a collocation method spatially and Newmark's method for time integration.[3]

Approximate solutions of the governing equations of the inclined cable with buoys are sought in the form of a truncated series.

$$F_N(s, t) = \sum_{n=1}^N f_n(t) b_n(s)$$

where

$F_N(s, t)$: approximate solution

$f_n(t)$: expansion coefficients of $F(s, t)$

$b_n(s)$: time independent orthogonal functions

For this expansion, Chebyshev polynomials $T_n(s)$ are used and they are orthogonal to each other in the interval $-1 \leq s \leq 1$, based on the collocation method for a spatial integration scheme. Due to nonconstant terms in the governing equations of the cable, the collocation method is superior to Galerkin's method [4].

3. Numerical Applications

The inclined cable GUYSTA is used in order to determine the effects on the dynamic response the principal parameters of the inclined cable are found in Table 1.

Fig. 2 shows the static configuration of the inclined cable. The natural frequencies of this cable are

First Natural Frequency = 0.900 rad/sec

Second Natural Frequency = 1.193 rad/sec

$T_p = 1332000\text{N}$	$L = 1036\text{m}$
$m = 48.7\text{kg/m}$	$Do = 0.0889\text{m}$
$m_a = 6.3\text{kg/m}$	$\text{depth} = 426.7\text{m}$
$W_{\text{water}} = 414.98\text{N/m}$	$Cdn = 1.2$
$EA = 1.3 \times 10^9\text{N}$	$Cdt = 0.05$
No current	

Table 1 Principal parameters of the inclined cable

The excitation is applied at the top point of the inclined cable, in the form of an imposed motion, whose amplitude is equal to 10 cable diameters and its frequency is equal to the first natural frequency of the cable.

Fig. (3), (4) and (5) show the dynamic response of the cable subjected to only the nonlinear drag forces and, in a few periods, the dynamic responses reach steady state. In Fig. (5), the high frequency fluctuations result from the strong singularity of the initial velocity.

Fig. (6), (7) and (8) show the dynamic response of the cable with geometric nonlinearity and large tensile forces, as well as nonlinear drag forces. The

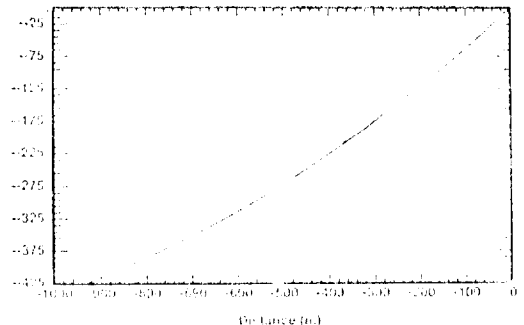


Fig. 2 Static configuration of GUYSTA

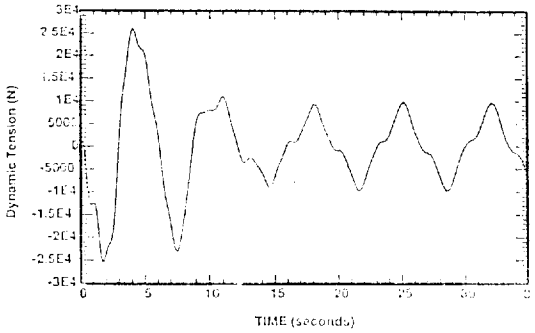


Fig. 3 Dynamic tension at the middle of GUYSTA, subjected to only nonlinear drag forces [10 diameters, 0.9rad/sec]

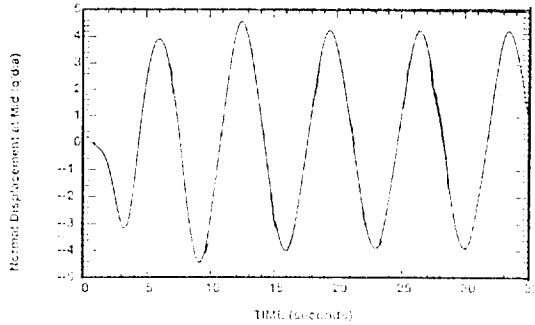


Fig. 4 Normal displacement at the middle of GUYSTA, subjected to only nonlinear drag forces [10 diameters, 0.9rad/sec]

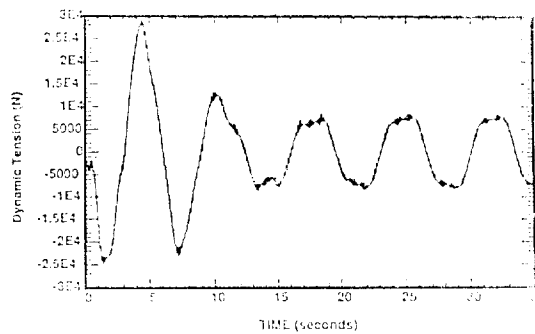


Fig. 5 Dynamic tension at the top of GUYSTA, subjected to only nonlinear drag forces [10 diameters, 0.9rad/sec]

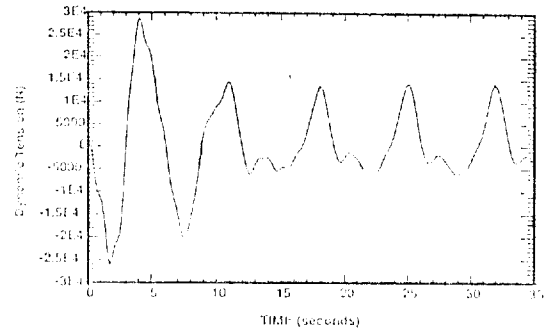


Fig. 6 Dynamic tension at the middle of GUYSTA, subjected to geometric nonlinearity and large tensile forces as well as nonlinear drag forces [10 diameters, 0.9rad/sec]

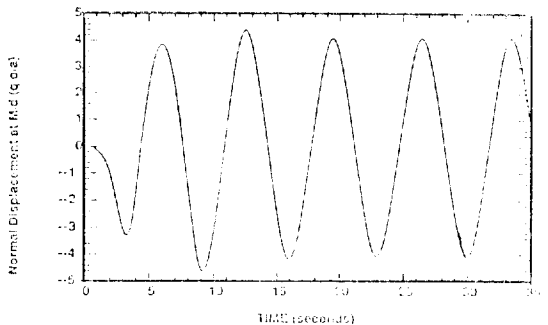


Fig. 7 Normal displacement at the middle of GUYSTA, subjected to geometric nonlinearity and large tensile forces as well as nonlinear drag forces [10 diameters, 0.9rad/sec]

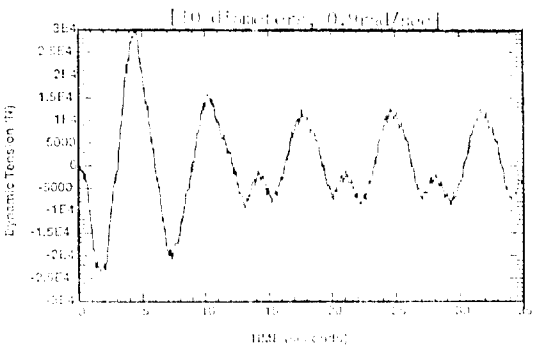


Fig. 8 Dynamic tension at the top of GUYSTA, subjected to geometric nonlinearity and large tensile forces as well as nonlinear drag forces [10 diameters, 0.9rad/sec]

combined effects of both geometric nonlinearity and large tensile forces on the dynamic tension are observed making small peaks between large peaks of the

dynamic tension in Fig. (6) and (8).

Through comparison between the dynamic response of the cable with only nonlinear drag forces and

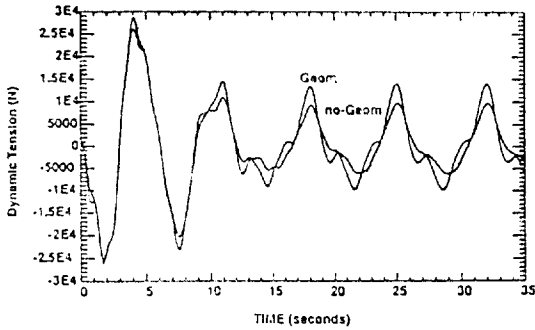


Fig. 9 Comparison between dynamic tensions at the middle of GUYSTA subjected to nonlinear drag forces and GUYSTA subjected to geometric nonlinearity and large tensile forces as well as nonlinear drag forces [10 diameters, 0.9 rad/sec]—from Figs. 3 and 6

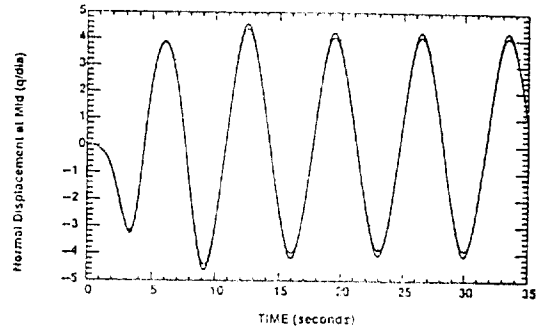


Fig. 10 Comparison between normal displacements at the middle of GUYSTA subjected to nonlinear drag forces and GUYSTA subjected to geometric nonlinearity and large tensile forces, as well as nonlinear drag forces [10 diameters, 0.9rad/sec]

Table 2 Comparison of the maximum dynamic response of GUYSTA with only nonlinear drag forces, with respect to the case of including both geometric nonlinearity and large tensile forces, as well as nonlinear drag forces

Item	Combined effects	Nonlinear drag forces only	Difference(%)
Maximum dynamic tension in the middle	14138.6N	9744.02N	+45%
Maximum normal displacement in the middle	4.282(m/dia)	4.10(m/dia)	+4.44%
Maximum dynamic tension at the top	12499.5N	8266.13N	+51.21%

that of the cable with the combined effects of geometric nonlinearity and large tensile forces in Fig. (9),(10) and (11), author found that, in steady state, the combined effects increase the maximum dynamic tension (Fig. 9 and 11) and reduce the magnitude of the minimum of the dynamic tension at the middle of the cable (Fig. 9). In table 2, the increase in the maximum dynamic tension at the middle of the cable was 45% and, the increase at the top 51%.

The decrease in the magnitude of the minimum dynamic tension in the middle of the cable is found to be equal to 36% (Table 3). This decrease, together with the increase of the maximum dynamic tension, cause the average tension to become higher.

The same phenomena-increase of the maximum and reduction of the magnitude of the minimum—are obtained for both the tangential and normal displacements (Fig. 10 and Table 2 and 3).

Table 3 Comparison of minimum dynamic responses of GUYSTA with only nonlinear drag forces with respect to the case of both geometric nonlinearity and large tensile forces, as well as nonlinear drag forces

Item	Combined effects	Nonlinear drag forces only	Difference(%)
Minimum dynamic tension in the middle	-6260.96N	-9779.85N	-36%
Minimum normal displacement in the middle	-3.917(m/dia)	-4.095(m/dia)	-4.3%
Minimum dynamic tension at the top	-8820.14N	-8262.12N	+6.7%

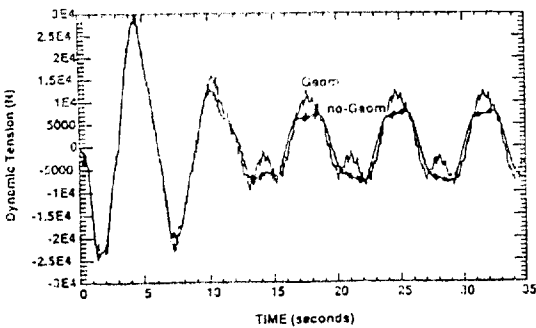


Fig. 11 Comparison between dynamic tensions at the top of GUYSTA subjected to nonlinear drag forces and GUYSTA subjected to geometric nonlinearity and large tensile forces, as well as nonlinear drag forces [10 diameters, 0.9 rad/sec]—from Figs. 5 and 8

4. Conclusions

Comparisons in Tables (2) and (3) means that, for this particular excitation, we should include the geometric nonlinearity and large tensile forces in order to estimate accurately extreme tensions. For higher frequencies and larger amplitudes of excitation, the contribution to the dynamic tension from large tensile forces,

and the geometric nonlinearity is expected to increase. This has serious effects on the fatigue life of the cable, necessitating the use of the present approach if reliable results are to be obtained.

References

- [1] Triantafyllou, M.S., Blik, A. and Shin, H. "Dynamic Analysis as a Tool for Open-Sea Mooring System Design", Transactions, The Society of Naval Architecture and marine Engineering (12), November, 1985.
- [2] Blik, A., "Dynamic Analysis of Single Span Cables". Ph.D thesis, MIT, 1984.
- [3] Bathe, K.J., "Finite Element Procedures in Engineering Analysis", Prentice Hall, Englewood Cliffs N.J., 1982.
- [4] Gottlieb, D. and Orszag, S.A., "Regional Conference Series in Applied Mathematics: Numerical Analysis of Spectral Methods, Theory and Applications", Society for Industrial and Applied Mathematics, Philadelphia, 1977.
- [5] Shin, H., "Nonlinear Cable Dynamics", Ph.D thesis, MIT, 1987.